$$\left.\frac{dY_{in}}{df}\right|_{f_0} = \left.\frac{dY_{in}}{dk}\right|_{k_0}\cdot\frac{k_0}{f_0} = \frac{j}{\eta}\cdot\frac{k_0^2r^2}{f_0(d/\lambda_0)}\cdot\left[\frac{RG_1(k_0r)}{rF_0(k_0r)} - 1\right] \quad (4)$$

where

$$G_1(kr) = J_1(kr)N_1(kR) - N_1(kr)J_1(kR). \quad (5)$$

For a uniform $\lambda/4$-transmission line

$$\left.\frac{dY_{in}}{df}\right|_{f_0} = j\cdot\frac{\pi}{2}\cdot\frac{1}{Z_0f_0} \quad (6)$$

where Z_0 is the characteristic impedance of the line. By setting the right-hand sides of (4) and (6) equal, the equivalent Z_0 of the radial antiresonant line may be solved. It becomes

$$Z_0 = \frac{\eta}{8\pi}\cdot\frac{d/\lambda_0}{(r/\lambda_0)^2}\cdot\frac{1}{\left[\frac{R}{r}\frac{G_1(k_0r)}{F_0(k_0r)} - 1\right]}. \quad (7)$$

In Fig. 2, the dependence of Z_0 on r/λ_0 is plotted in the case of the lowest antiresonance. In the same diagram, the characteristic impedance of a strip line with a strip width equal to the mean circumference of the radial line is also presented for comparison. In both cases, a distance d of $\lambda/10$ and air filling is assumed but the results may easily be calculated for other distances and fillings, by multiplying with $d/0.1\lambda$ and dividing with $\sqrt{\epsilon_r}$, as is seen from (7). For solving the equation $F_1(k_0r)=0$, we refer to a diagram in [2]. The Q of the resonator, calculated by definition (8), leads to (9).

$$Q = \frac{\omega_0\cdot\text{energy stored in the resonator}}{\text{average power loss in the walls}} \quad (8)$$

$$Q = \frac{\omega_0\epsilon\eta^2d}{R_s}\cdot\frac{\int_r^R rF_0^2(k_0r)dr}{\left[2\int_r^R rF_1^2(k_0r)dr + RdF_1^2(k_0R)\right]} \quad (9)$$

R_s is the surface resistance of the resonator material at the given frequency. For a linear combination F_p of Bessel and Neumann functions of order p

$$\int rF_p^2(kr)dr = \frac{r^2}{2}\left[F_p^2(kr) - F_{p-1}(kr)F_{p+1}(kr)\right] \quad (10)$$

is valid. Noting that $F_1(k_0r)=0$ and $F_0(k_0R)=0$ we see that

$$\int_r^R rF_1^2(k_0r)dr = \int_r^R rF^2{}_0(k_0r)dr$$

$$\left[= \frac{1}{2}R^2F_1^2(k_0R) - r^2F_0^2(k_0r)\right], \quad (11)$$

thus giving the value of Q:

$$Q = \frac{\omega_0\epsilon d\eta^2}{2R_s}\cdot\left[\frac{R^2F_1^2(k_0R) - r^2F_0^2(k_0r)}{R(R+d)F_1^2(k_0R) - r^2F_0^2(k_0r)}\right]. \quad (12)$$

The factor in brackets is practically a constant depending on values of d only and can be approximated with $R/(R+d)$, the error being within a few percent. This is the case of the cylindrical resonator ([3], p. 428) and can directly be deduced from (12) by omitting the terms with r.

ISMO V. LINDELL
Radio and Electronics Lab.
Dept. of Elec. Engrg.
Institute of Technology
Helsinki, Finland

REFERENCES

[1] B. C. De Loach, Jr., "Radial-line coaxial filters in the microwave region," *IEEE Trans. on Microwave Theory and Techniques*, vol. MTT-11 pp. 50–55, January 1963.
[2] *The Microwave Engineers' Handbook 1965*. New York: Horizon House-Microwave Inc., p. 54.
[3] S. Ramo and J. R. Whinnery, *Fields and Waves in Modern Radio*. 2nd ed., New York: Wiley, 1953.

A Novel Strip-Line Circulator

A circulator with strip-line inputs has been developed which incorporates a single disk of yttrium aluminum iron garnet (YAIG) on one side of the center conductor and a large, metallic short circuit on the other side. The short circuit can be the magnet necessary to bias the garnet to the optimum field for broadband circulation. The basic design is shown in Fig. 1. The center conductor junction is round with alumina loaded quarter-wave transformer coupling to the 50-Ω input lines. Compared to a standard circulator with two YAIG disks operating in the same frequency range, the center conductor diameter is somewhat larger and the transformers of somewhat lower impedance. The metallic disk is smaller than the center conductor diameter and is one of the factors which determine the resonant frequency of the junction. The performance of a typical unit is plotted in Fig. 2. This isolation characteristic is double humped and ranges from 30 to 40 dB across a 13.7 percent frequency band. The insertion loss is 0.2 dB across the same band.

In order to understand the modal configuration which allows circulation to exist in this design, a completely air loaded two-port transmission structure was built as shown in Fig. 3. The junction diameter was kept the same as the circulator. A large number of small diameter probing holes were included in the walls and the fields were examined at the resonant frequencies of the structure. The lowest mode occurs at 1.48 GHz. The magnetic field lines are concentric circles about the axis of symmetry. The maximum "h" field intensity occurs around the short-circuiting disk and continuously decreases to a minimum at the center of the opposite side of the structure. This mode, by itself, cannot be used for circulation. In a three-port structure, with the ferrite and alumina in place, the mode would occur at approximately one third the frequency of the circulator. The mode of interest for circulation was found at 4.92 GHz and has the field pattern of Fig. 4. This pattern is similar to the dipolar mode described by Fay and Comstock.[1] In a symmetrical three-port configuration with a magnetized ferrite disk in the junction region, this pattern can be rotated in the proper manner for circulation.

It is also possible to extend this matching

Manuscript received October 6, 1965.

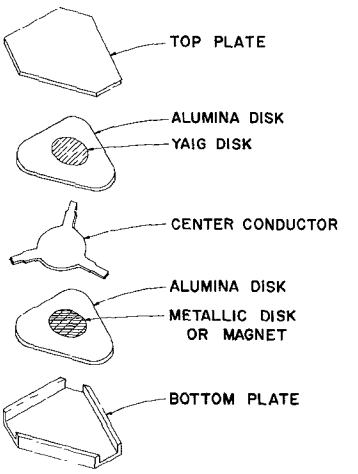

Fig. 1. Exploded view of a three-port circulator with metallic short between the center conductor and ground.

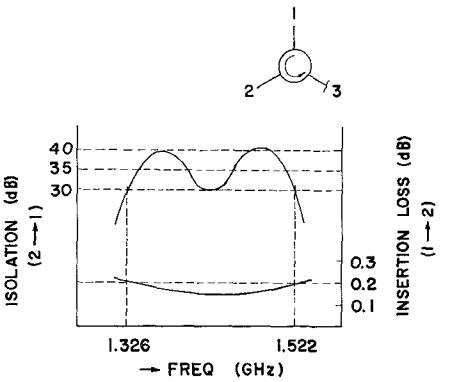

Fig. 2. Isolation and insertion loss characteristics of the circulator.

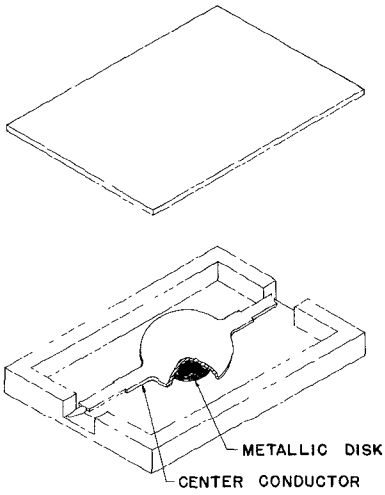

Fig. 3. Two-port air loaded resonant structure.

[1] C. E. Fay and R. L. Comstock, "Operation of the ferrite junction circulator," *IEE Trans. on Microwave Theory and Techniques*, vol. MTT-13,pp. 15–27 January 1965.

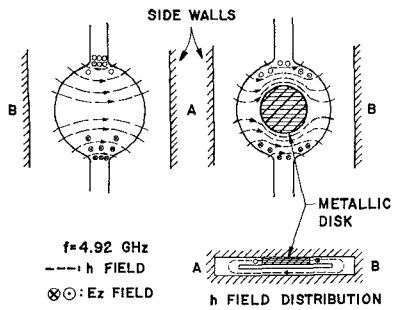

Fig. 4. Field patterns of the mode of interest for circulation.

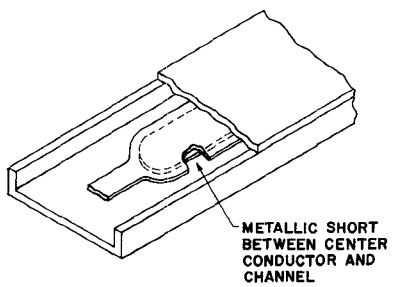

Fig. 5. Folded waveguide structure with strip-line input.

solution to the folded waveguiding structure shown in Fig. 5. The dominant mode in this structure has a TE_{10} like pattern which is folded back on itself at both sides of the waveguide. Some of the characteristics of this waveguide are the following: 1) Because of the reduced aspect ratio, the waveguide is low impedance. 2) The cutoff frequency is considerably reduced compared to a standard waveguide of similar external dimensions. 3) It is relatively simple to match into this waveguide from in-line coax or strip line. In addition to being useful for circulator design, this field configuration permits the design of broadband waveguide-type components with simple in-line coaxial terminals.

M. D. Bonfeld
D. F. Linn
M. Omori
Bell Telephone Labs., Inc.
Allentown, Penn.

On Nonresonant Perturbation Measurements

A perturbation measurement technique has been developed at Stanford University which determines the phase and field strength at a point inside a microwave structure by measuring the reflection produced at the input port by a perturbing bead. The theoretical basis for the measurement is presented in this issue by C. Steele [1]. Some applications and experimental considerations of the technique are presented here.

Manuscript received October 11, 1965. The work reported in this paper was supported by the U. S. Atomic Energy Commission.

A typical experimental setup is shown schematically in Fig. 1. Since the quantity of interest is the change of reflection due to the perturbation, the slide-screw tuner is used to tune out reflections before inserting the bead. The difference of the crystal currents is proportional to $A^2|\Gamma|\cos\phi$, where A is the amplitude of the reference signal from the generator, Γ is the reflection of the bead and ϕ is its phase. The phase of Γ for each bead location is determined by setting the precision phase shifter to achieve a null signal and the reflection amplitude by measuring the maximum unbalance signal. For a dielectric bead, Steele shows that $\Gamma = k\,E^2\exp(2i\theta)/P_i$, where E and θ are the amplitude and the phase of the electric field at the bead and P_i is the input power. While the constant k is calculable for simple solids of revolution, it is often more convenient to calibrate a bead in a structure of known properties such as the uniform input waveguide to the test structure or a cavity consisting of a right circular cylinder.

As with any perturbation measurement, the perturbation must be small. The magnitude of the reflection coefficient must be much less than unity and the product of the propagation constant associated with any coordinate by the length of the bead along that coordinate must be much less than unity (i.e., the bead must be much smaller than a wavelength). Furthermore, to avoid image effects, the distance from the walls of the structure to the bead must be large compared with the bead dimensions.

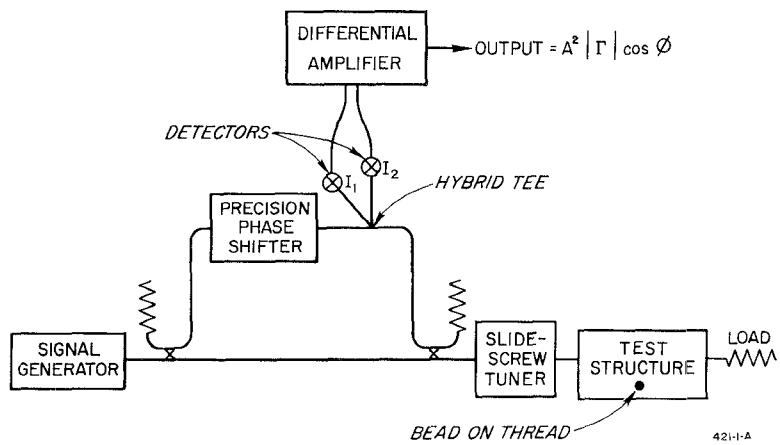

Fig. 1. Reflection perturbation measurement.

The technique is most useful in traveling-wave structure in which either 1) the structure is sufficiently irregular that the standing-wave pattern produced by resonating the structure masks the significant phase and field strength distributions, or 2) the loss is so high that the structure will not support a resonance of high Q-factor, well-separated from adjacent resonances.

One example of the first type was the measurement of fields in a high-power waveguide vacuum valve developed at Stanford Linear Accelerator Center. The technique was used by R. P. Borghi to measure the peak fields in the valve, thus determining the high power-handling capability.

Another example is the measurement of the symmetry properties of the couplers for the SLAC accelerator sections. Although the accelerator section itself has cylindrical symmetry, the power is fed into the coupler from a waveguide iris on one side. An electron passing through an accelerator section is given a transverse impulse proportional to the line integral along the electron path of the quantity $j\partial E_z/\partial x$, where the complex quantity E_z is the coupler field. The measurement of the phase was made by R. P. Borghi and G. A. Loew with a precision of about 0.1° using the technique described before. A transverse phase shift of about 1° was observed, which was large enough to require design changes in the SLAC accelerator [2].

In waveguide two-ports, an additional useful measurement may be made. The perturbing bead may be represented as a shunt susceptance which introduces equal forward- and back-scattered waves in a running wave. The back-scattered wave is observed at the input; as shown by Steele, it is a measure of the square of the field, normalized to the input power. The forward-scattered wave is observed as a phase shift at the output; it is a measure of the square of the field intensity, normalized to the power flux at the bead [3], [4]. The ratio of the two is a measure of the attenuation from the input port to the bead.

The reflection and the transmitted phase-shift techniques were used by the authors to calibrate a mockup of the tapered disk-loaded bunching section of an X-band electron linear accelerator buncher.[1]

Measurement of the reflection from a perturbing bead allowed direct determination of the phase velocity and field strength on the axis of the structure. The ratio to the measurement of transmitted phase shift allowed a check of the predicted value of attenuation. Errors of phase velocity, field strength, and internal matching were disclosed in the calibration measurements of the mockup. Small corrections were computed and the final accelerator was constructed and remeasured.

[1] The phase velocity was to vary from 0.5 c to 1.0 c in the first five wavelengths of the structure. The field strength was to increase by a factor of 7 in the same distance.